from the two levels involved in an optical transition.

Finally, it is interesting to compare our result (28) with the one obtained from nuclear-Coulomb-excitation measurements. Collective nuclear-model calculations show that the transition probability for an electric-dipole transition between two nuclear levels I_i and I_f in the same rotational band is given by[16]

$$B(E2; I_i \rightarrow I_f) = (5/16\pi)\, e^2 Q_1^2 \Omega^2, \tag{29}$$

where B is the transition probability, $E2$ designates it as an electric-dipole transition, e is the electronic charge, Q_1 is the intrinsic nuclear quadrupole moment, and Ω is a matrix element connecting the two states.

The intrinsic quadrupole moment Q_1 is related to the quadrupole moment Q_0 in the nuclear ground state by[16]

$$Q_1 = Q_0 \frac{I(2I-1)}{(I+1)(2I+3)} \ . \tag{30}$$

It follows then that if one compares transition probabilities between states I_i and I_f for Gd^{155} and Gd^{157}, where I, I_i, and $I_f \equiv I$ are the same in both isotopes,

$$[B(E2)^{155}/B(E2)^{157}]^{1/2} = Q_0^{155}/Q_0^{157}. \tag{31}$$

From the tables of Alder *et al.*[16] we have

$$B(E2; \tfrac{5}{2} \rightarrow \tfrac{3}{2})^{155}/B(E2; \tfrac{5}{2} \rightarrow \tfrac{3}{2})^{157} = 3.3/3.5.$$

The square root of this ratio is 0.97, in very good agreement with our result.

*Present address: Department of Electrical Engineering, University of Southern California, Los Angeles, Calif. 90007.

[1]H. G. Kahle, V. Koch, J. Plamper, and W. Urban, J. Chem. Phys. 49, 2702 (1968).
[2]W. Urban, J. Chem. Phys. 49, 2703 (1968).
[3]J. Rosenthal, R. F. Riley, and U. Ranon, Phys. Rev. 177, 625 (1969).
[4]See Refs. 2 and 3 for discussion of the crystal-field parameters and further references.
[5]See, e.g., W. Low, in *Solid State Physics*, edited by F. Seitz and D. Turnbull (Academic, New York, 1960), Suppl. 2.
[6]R. W. G. Wyckoff, *Crystal Structures* (Interscience, New York, 1965), Vol. 3.
[7]M. T. Hutchings, Solid State Phys. 16, 227 (1965), and references therein.
[8]See, e.g., U. Ranon and J. S. Hyde, Phys. Rev. 141, 259 (1966).
[9]J. Rosenthal, Phys. Rev. 164, 363 (1967).
[10]B. Bleaney, Phil. Mag. 42, 441 (1951).
[11]J. M. Baker, G. M. Copland, and B. M. Wanklyn, J. Phys. C 2, 862 (1969).
[12]I. Lindgren, Arkiv Fysik 29, 553 (1965); see also V. S. Shirley, in *Hyperfine Structure and Nuclear Radiation*, edited by E. Matthias and D. A. Shirley (North-Holland, Amsterdam, 1968), table of nuclear moments.
[13]A. J. Freeman and R. E. Watson, Phys. Rev. 127, 2058 (1962).
[14]D. R. Speck, Phys. Rev. 101, 1725 (1956).
[15]N. I. Kaliteevskii, M. P. Chaika, I. Kh. Pacheva, and E. E. Fradkin, Zh. Eksperim. i Teor. Fiz. 37, 882 (1959) [Soviet Phys. JETP 10, 629 (1960)].
[16]K. Alder, A. Bohr, T. Huus, B. Mottelson, and A. Winther, Rev. Mod. Phys. 28, 432 (1956).

PHYSICAL REVIEW B VOLUME 3, NUMBER 7 1 APRIL 1971

Stopping Cross Sections for Fission Fragments of ^{252}Cf by Gold, Silver, and Carbon†*

L. Bridwell and A. L. Walters, Jr.
Department of Physics, Murray State University, Murray, Kentucky 42071
(Received 10 August 1970)

Using ^{252}Cf as a source of heavy ions, the stopping cross sections were determined for stopping media of gold, silver, and carbon. The dependence of stopping cross sections on the nuclear charge of the heavy ions was observed at approximately 1.3 cm/nsec. The results are in reasonable agreement with the theory by Lindhard. In some cases, better agreement can be obtained by using a formula published earlier by Bridwell and Moak.

I. INTRODUCTION

During the past few years technological developments, such as the transuranic heavy-ion accelerator, certain chemonuclear systems, and the fission electric cell have created the need for more information concerning energy loss by heavy ions in various types of stopping materials. The differential energy loss or the stopping power of a material, is the amount of kinetic energy lost per unit path length and is given by the formula

$$-\frac{dE}{dx} = n\sigma, \tag{1}$$

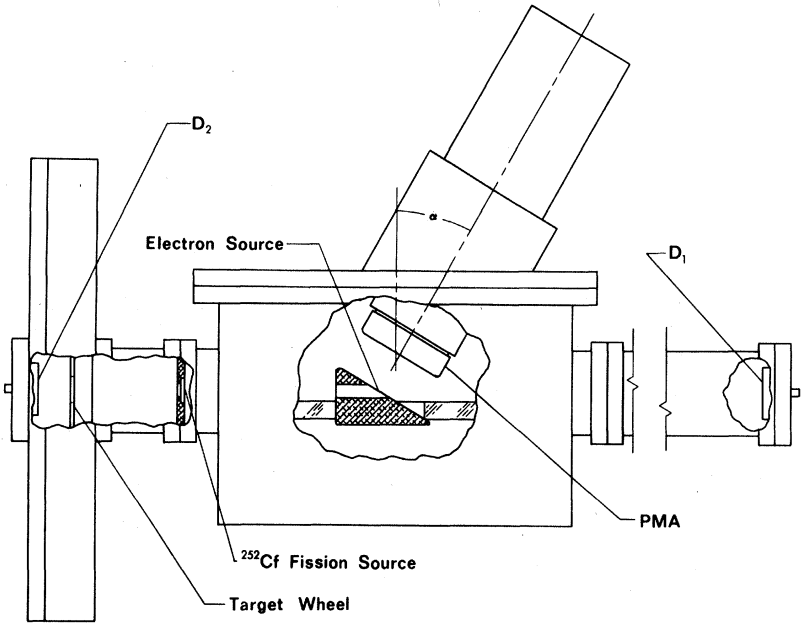

FIG. 1. Experimental system showing the two fission-fragment detectors D_1 and D_2, the fission source, the photomultiplier assembly, PMA, of the secondary electron system, and the target foil wheel all inside the vacuum chamber.

where n is the atomic particle density of the stopping medium, and σ is the stopping cross section for each atom given in units of eV cm^2. Past work, such as that by Bohr, [1] predict ranges for heavy ions in media of various atomic numbers. In a more recent approach, Lindhard *et al.* [2] concluded that the differential energy loss for an ion was dependent on its nuclear charge and not on its initial state of ionization.

In some recent experiments, such as that by Moak *et al.*, [3] stopping-power data have been obtained for several types of stopping media which are supported by the latest theory by Lindhard *et al.* [2] Experiments of this nature, however, are limited with respect to the variation of ions available. Other results using fission fragments have been compared to a semiempirical theory based on an effective ionic charge. [4]

The present work, by its use of a spontaneous fissioning source, provides a more versatile study of the behavior of stopping powers and stopping cross sections as a function of the mass or atomic number of the incident ion.

II. EXPERIMENTAL PROCEDURE

The experiment used to determine the stopping powers as a function of mass had three parameters involved. The energy of the primary fission fragment (E_1) and the time necessary for it to traverse a measured distance (t_{0f}) were used to determine

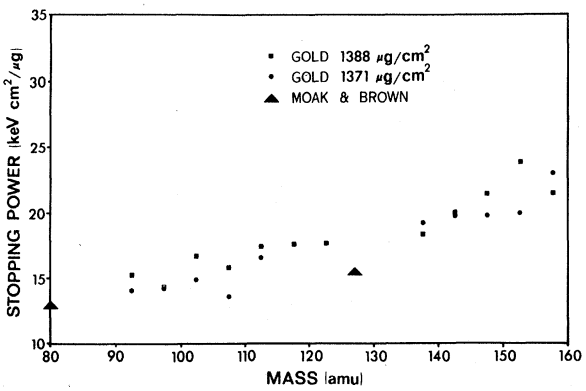

FIG. 2. Observed stopping power of gold vs the fission-fragment mass appropriately adjusted to the velocity of the most probable light fragments (1.32 cm/nsec).

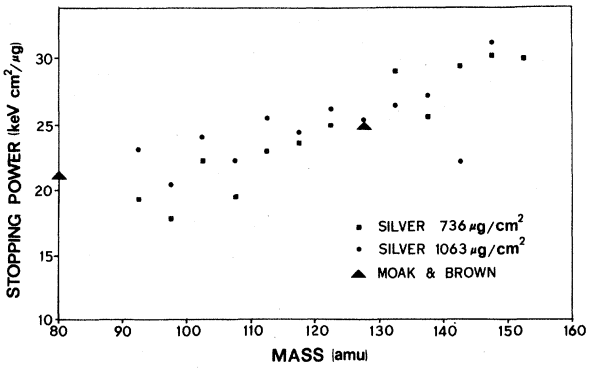

FIG. 3. Observed stopping power of silver vs the fission-fragment mass appropriately adjusted to the velocity of the most probable light fragments (1.35 cm/nsec).

masses in the fission event. The energy of the complementary fragment (E_2) was then studied to determine the energy loss in a particular target foil.

The schematic illustration for the system used in this multiparameter experiment is shown in Fig. 1. The two silicon-gold surface-barrier detectors D_1 and D_2, the source, the target foil, and the foil holder in the center of the chamber were aligned to obtain optimum counting geometry. The plastic scintillator, covered with a wire grid, was placed about 2 cm from the foil holder so as not to obstruct the fission fragment path. A negative voltage of 15 kV with respect to the wire grid, was placed on the foil holder to accelerate the secondary electrons from the foil past the wire grid into the scintillator. The foil used was made from carbon and was approximately 5-μg/cm^2 thick. During data acquisition, the fission chamber was kept at a vacuum of approximately 10^{-6} Torr.

The source, ^{252}Cf, was mounted on one side of a thin nickel foil of approximately 200-μg/cm^2 thick, which gave a two-sided source. The target foils of gold, silver, and carbon were obtained by the technique of vacuum deposition. Their thicknesses were measured by α-ranging procedures using tables and formulas by Whaling.[5]

When ^{252}Cf fissioned, the following events took place. One fragment, with mass m_1 and energy E_1, traveled to the right and encountered the secondary electron foil. The energy loss in the foil was small but secondary electrons were emitted and detected by the photomultiplier assembly (PMA). The electron foil marked the beginning of the measured distance and the PMA pulse marked the starting time t_1. At the end of the path, D_1 measured the energy E_1 of the fragment m_1 and marked the ending time t_2. A simultaneous emission of the complementary fragment m_2 occurred with the emission of m_1. The path of m_2 was to the left. The complementary fragment suffered an energy loss if a target was in position, after which it was detected by D_2. The signals from the PMA and D_1 were then routed through an appropriate selection of delays to the time-to-pulse-height converter (TPHC). The time pulse along with the two energy pulses were sent to individual analog to digital converters. The accompanying gate pulse, initiated by the time and energy pulses being in triple coincidence, allowed an event to be processed by CINDA[6] operated in the three-parameter mode.

According to Schmitt *et al.*,[7] the energy signal from a surface-barrier detector is linear for fission fragments having kinetic energies up to 100 MeV. This range of values was later extended to 200 MeV by Bridwell *et al.*[8] Schmitt expressed the relationship between the kinetic energy of the particular fragment and the measured pulse height from the energy detector by the equation

$$E = (a + a'm)x + (b + b'm), \tag{2}$$

where

$$a = 24.0202/(P_L - P_H),$$

$$a' = 0.03574/(P_L - P_H),$$

$$b = 89.6083 - aP_L,$$

$$b' = 0.1370 - a'P_L.$$

P_L and P_H are the peak positions of the light and heavy fission fragments, and x is the energy pulse height as determined from a fission fragment kinetic-energy spectrum. The measured time was not the true time of flight owing to system delays. Appropriate corrections in time were made for these delays. Having found t_{0f}, then the Eq. (2) along with

$$E_1 = \tfrac{1}{2}m_1 v_1^2 = m_1 d^2/2t_{0f}^2 \tag{3}$$

gave an expression from which a mass number was calculated for each event. The mass of the complementary fragment m_2 was calculated by assuming an average of three prompt neutrons from each fission event. Thus

$$m_2 = 252 - 3 - m_1. \tag{4}$$

By using the calculated mass m_2, the energy of the complementary fragment was calculated using Eq. (2). The events were then sorted for the energy of the complementary fragment whose masses fell in 5-amu bins in the range 90–160 amu.

The energy spectrum for each mass bin displayed a prominent peak whose energy value was taken to be the most probable energy $[E(m)]$ for that mass. These spectra were obtained for each of the absorber foils as well as for several open runs. The difference between the most probable energy $E(m)$ and the most probable energy for the

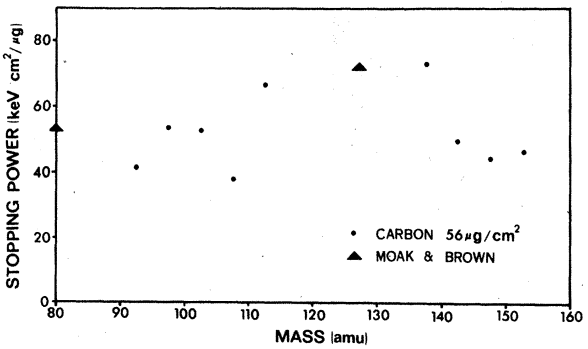

FIG. 4. Observed stopping power of carbon vs the fission-fragment mass appropriately adjusted to the velocity of the most probable light fragments (1.38 cm/nsec).

same mass of the open run determined $\Delta E(m)$ for each foil for each mass bin. Using these values for $\Delta E(m)$ and the foil thickness values, as obtained by α-ranging techniques, associated stopping powers were found for a particular target foil. It is well known that at fission fragment energies the stopping power is velocity dependent.[2,9,10] To make a comparison of stopping powers for different projectiles it was necessary to adjust the measured stopping powers for the different velocities. Thus

$$\left(\frac{dE}{dx}\right)' = \left(\frac{dE}{dx}\right)\frac{v'}{v} ,$$

where dE/dx is the measured stopping power, v' is the velocity of the particular fragment group, and v is the average velocity of the most probable light fragment which was approximately 1.3 cm/nsec in each ease. Results from the work by Moak and Brown[9] are included for comparison.

For ions in the energy range under consideration, 60–100 MeV, the dominating factor in the total stopping cross section of a material is σ_e the stopping cross section of the atomic electrons. According to Lindhard *et al.*,[3] σ_e, for a projectile having a velocity v, is given by the equation

$$\sigma_e = 8\pi a_0 \xi_e e^2 (Z_1 Z_2 / Z)(v/v_0) , \qquad (5)$$

where

$$Z = (Z_1^{2/3} + Z_2^{2/3})^{3/2} ,$$

$$\xi_e \simeq Z_1^{1/6} .$$

The subscripts 1 and 2 refer to the projectile and stopping media, respectively, while a_0 and v_0 are the radius of the first Bohr orbit and the corresponding velocity of an electron in the first Bohr orbit. From Eqs. (1) and (5) it follows that

$$m\frac{dE}{dx} \Big/ \frac{Z_2 v}{v_0} = \xi_e \frac{8\pi e^2 a_0 Z_1}{Z} , \qquad (6)$$

where dE/dx is the observed stopping power associated with the selected mass group, and Z_1 is the most probable post-neutron-emission atomic number of the projectile. Each Z_1 was obtained by choosing a median mass number for each mass bin and applying the equal charge displacement rule (Glendenin's rule[11]). The normalized stopping cross sections were plotted as a function of Z_1 and compared to theoretical values as obtained from Eq. (6).

Earlier work yielded an empirical expression for the stopping power for heavy ions.[11] Stopping cross sections were calculated from this and compared to the experimental data and Lindhard's work.[3]

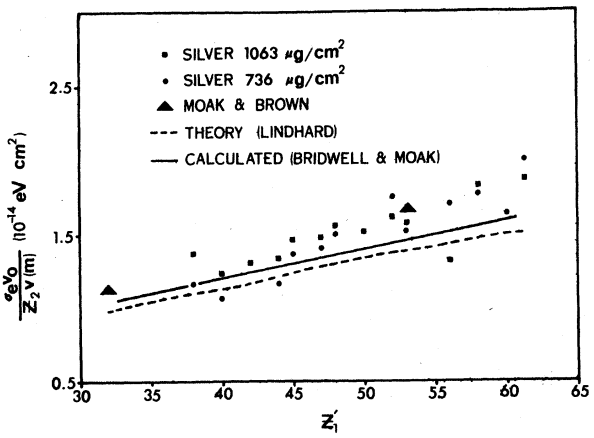

FIG. 6. Normalized stopping cross section of silver vs fission-fragment atomic number.

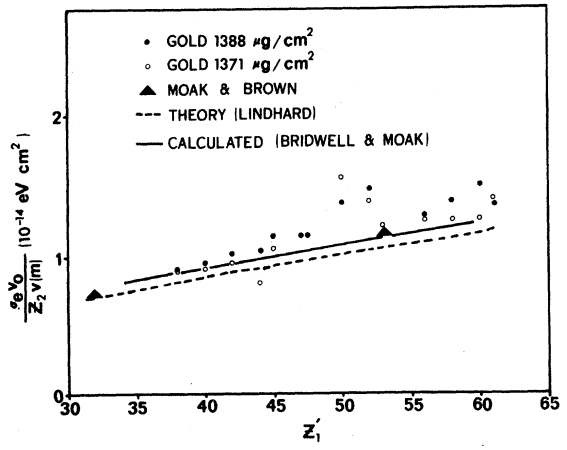

FIG. 5. Normalized stopping cross section of gold vs fission-fragment atomic number.

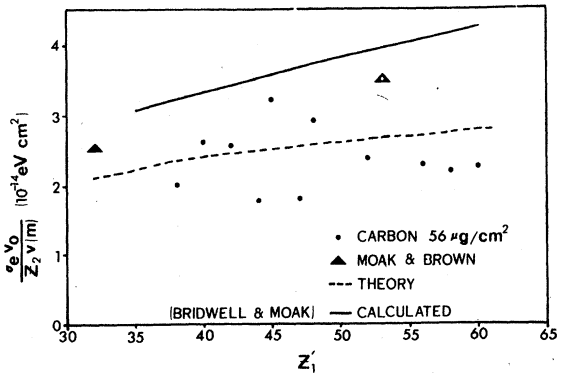

FIG. 7. Normalized stopping cross section of carbon vs fission-fragment atomic number.

III. RESULTS

Mass numbers for the fission fragments of ^{252}Cf have a value such that $90 \leq m \leq 160$. The resulting stopping-power plots as obtained by successive application of Eqs. (2) and (4) and normalizing to the velocity of the most probable light fragment are shown in Figs. 2–4. In some cases such as on the boundaries and in the mid-region of the mass range, the resulting energy points were not available due to poor statistics in the raw experimental data. The bromine and iodine ion data, as obtained by Moak *et al.*,[9] shown on the same plots are in reasonable agreement for all materials.

Figures 5–7 show the results of the normalized stopping cross sections as a function of the projectile atomic number Z_1. Included on the graphs are points obtained by Moak *et al.*[9] and the theoretical prediction by Lindhard *et al.*[3] The solid line is from the empirical relationship mentioned earlier.[10] The errors in the data resulting from a statistical uncertainity are estimated to be about 25–30% full width at half-maximum (FWHM) for Au and Ag and somewhat larger for C. Analysis of the raw data was rather involved making precise estimates of the errors difficult. The maximum probable error in the mass determination was about 4 amu. Thus the choice of the size of mass bin was 5 amu. An inspection of the figures will show that the data are consistant with the estimated errors.

The characteristic behavior of the Au and Ag data indicates that the theory is incomplete especially for the high-mass fragments. Statistical uncertainties in the carbon data prevent the drawing of any definite conclusions. One possible reason for the discrepancies is that internal excitation is not accounted for in the theory and may be much greater in the heavier ions.

†Research supported by the U. S. Atomic Energy Commission.

*Much of this material is contained in a Master's thesis by one of the authors (A. W.) as submitted to the Graduate School, Murray State University.

[1]N. Bohr, Kgl. Danske Videnskab. Selskab, Mat.-Fys. Medd. 18, No. 8 (1948).

[2]J. Lindhard, M. Scharff, and H. E. Schiott, Kgl. Danske Videnskab. Selskab, Mat.-Fys. Medd. 33, No. 14 (1963).

[3]C. D. Moak, H. O. Lutz, L. B. Bridwell, L. C. Northcliffe, and S. Datz, Phys. Rev. 176, 427 (1968).

[4]J. B. Cumming and V. P. Crespo, Phys. Rev. 161, 287 (1967).

[5]W. Whaling, *Handbuch der Physik* (Springer-Verlag, Berlin, 1958), Vol. 34, p. 193.

[6]J. Asbell (unpublished); L. Bridwell and L. M. Beyer, Bull. Am. Phys. Soc. 13, 1444 (1968).

[7]H. W. Schmitt, W. M. Gibson, J. H. Neiler, F. J. Walter, and J. D. Thomas, *Proceedings of the Symposium on the Physics and Chemistry of Fission, Salzburg*, 1965 (International Atomic Energy Agency, Vienna, Austria, 1965).

[8]L. B. Bridwell, L. C. Northcliffe, S. Datz, C. D. Moak, and H. O. Lutz, Bull. Am. Phys. Soc. 12, 28 (1967).

[9]C. D. Moak and M. D. Brown, Phys. Rev. 149, 244 (1966).

[10]L. Bridwell and C. D. Moak, Phys. Rev. 156, 242 (1967).

[11]L. E. Glendenin and J. P. Unik, Phys. Rev. 140, B1301 (1965).

PHYSICAL REVIEW B VOLUME 3, NUMBER 7 1 APRIL 1971

Electron Paramagnetic Resonance of Mn^{2+} in $KTaO_3$

David M. Hannon
IBM Research Laboratory, San Jose, California 95114
(Received 9 September 1970)

The electron paramagnetic resonance of Mn^{2+} in $KTaO_3$ was measured over a temperature range 4–110 K. At 77 K, the spin-Hamiltonian constants are $g_{\parallel} = 2.000 \pm 0.001$, $g_{\perp} = 2.000 \pm 0.001$, $D = +0.147 \pm 0.003$ cm^{-1}, $A_{\parallel} = -(86.5 \pm 0.5) \times 10^{-4}$ cm^{-1}, $A_{\perp} = -(84 \pm 1.5) \times 10^{-4}$ cm^{-1}. The results indicate that the Mn^{2+} is substitutional at a Ta^{5+} site with an adjacent oxygen vacancy. The temperature dependence of D is correlated with the soft-mode frequency of the host. The quadrupole splitting $Q' = +(0.8 \pm 0.1) \times 10^{-4}$ cm^{-1} was determined from the forbidden hyperfine transitions.

I. INTRODUCTION

This paper presents the electron paramagnetic resonance (EPR) of Mn^{2+} in the cubic perovskite $KTaO_3$, and is the first of two papers describing the spectroscopy of manganese in this host. It is